X-Ray Fluorescence

Eric Reichwein
Bryce Burgess
Department of Physics
University of California, Santa Cruz

February 3, 2014

Abstract

We examined the X-Ray fluorescence of zinc ($Z = 28$), copper ($Z = 29$), indium ($Z = 49$), gadolinium ($Z = 64$), erbium ($Z = 68$), and lead ($Z = 82$) and 3 unknown samples. After calibration we determined the samples to be iron, brass, and stainless steel using the characteristic X-rays and well established X-ray data tables. We then took our data tables and plotted the energies as a function of Z. Just as Moseley did we fit the data to the fit function $E(Z) = A(Z - \sigma)^2$ for the K_α lines. We looked into two different cases for the electron screening term $\sigma = 1$ or σ is free parameter. For the former we found the best fit was when $A = 11.7 \pm 0.1eV$. The latter case gave a fit of $A = 10.40 \pm 0.03eV$ and $\sigma = -0.99 \pm 0.04eV$. In the appendix we also present the fit for the L_α lines.

Contents

1 Introduction

This experiment is designed to emulate the discovery of Moseley's Law. We will first determine the X-ray spectra of six known and three unknown elements and verify them against our data tables. Then we will use our data tables of the binding energies to find the best parameter values for our fit function (see Eq. 1).

1.1 Historical Background

British physicist and chemist Henry Moseley first used X-ray fluorescence to make sense of the periodic table of elements in 1913. By shooting X-rays at certain compounds he observed unique spectra lines of the outgoing X-rays for each compound. He noted that the characteristic X-rays for each element had an order to it. This order was already well known by Dimitri Mendeleev's periodic table of elements. Moseley was able to mathematical and give physical description of the order of almost all available elements at the time, including nickel and cobalt[1] in the periodic table and predict two elements that had not been discovered yet ($Z = 72$ and $Z = 75$).

Unfortunately, Henry Moseley was shot in the head by a sniper during World War I. Moseley was 28 years old. Ernest Rutherford[2] and many others have said that he surely would have been given the Nobel prize for his work[2]. Neils Bohr commented that Moseley's work is truly what sparked the significant progress made in understanding the atom and not the work of Ernest Rutherford. His work was significant proof that quantum mechanics of atomic physics was indeed true. For it showed that all atoms of a specific element had the same quantized binding energies for its electrons.

1.2 Physics of X-Ray Fluorescence

Electrons exist in orbital clouds around a nucleus. The larger the nucleus the more electrons there are around it. Each orbital has a distinct potential or binding energy of the atom. All atoms have the same orbitals [3], but due to different number of electrons and protons, orbitals of dissimilar atoms have different energies. If an electron makes a transition between these states energy is released in the form of photons. These photons have a specific energy for each transition so we can exploit this to determine the electronic composition of different substances.

To do this we must first create a vacancy in an inner orbital. This is done by shooting X-rays at the substance of high enough energy to fully eject the electron from the atom (photoelectric effect), which can be seen in Fig. 1(a). After the high energy photon ejects an inner electron the remaining electrons naturally want to transition into the vacant orbital

[1]Nickel ($Z = 27$) and Cobalt ($Z = 28$) would have been incorrectly swapped if blindly placed by atomic mass (instead of atomic number) on the periodic table. However, Mendeleev knew that would be the case and correctly placed them and Moseley was able to physically describe why they must be swapped.

[2]Nobel prizes are not given post-humously. One exception is that of Immunologist Ralph Steinman for Medicine. He died hours after getting the call that he had won the Nobel prize. He has been the only post-humuous Noble prize recipient.

[3]By this statement, we mean that atoms of say $Z = 2$ and $Z = 3$ both have the $1s^2$ orbital in common.

because it is of lower energy. During the transition the characteristic X-ray is released. The type of X-ray is categorized by what orbital the vacancy is and what orbital the replacing electron started in. Referring to Fig. 1(b) we see that there is two possibilities shown, either the K_α or K_β X-rays. The letter states what the final orbital of the electron (that produced the X-ray) is and the subscript tells you how many orbitals it crossed to transition to the vacancy. The subscript is given a Greek letter but it corresponds to $\alpha = 1$, $\beta = 2$, $\gamma = 3$, and so on.

Figure 1(c) shows the "waterfall effect" or the possibility of the original photon not ejecting the inner most electron(s). We see that once the original vacancy is filled by an electron it creates another vacancy. It therefore will have an even higher energy electron transition into its vacancy and create another characteristic X-ray. However, these X-rays are the L lines because the final orbital of the transitioning electron is the L orbital. The vacancy will propagate itself until it is in the valence orbital. Analyzing the spectrum of these characteristic X-rays shows one how the electron cloud orbitals are distributed around any substance.

Figure 1: Diagram of X-ray fluorescence. [5] (a) A high energy photon ejects one of the inner electrons creating a vacancy. (b) The vacancy is then filled by electrons of higher energy orbitals. The transitions produce X-rays characteristic of to that element because of the unique energy differences between orbitals in each atom. (c) The filling of vacancies cause a waterfall effect. The vacancy is now in the next highest orbital (L) and higher orbital electrons will transition into the new L vacancy and produce more characteristic X-rays.

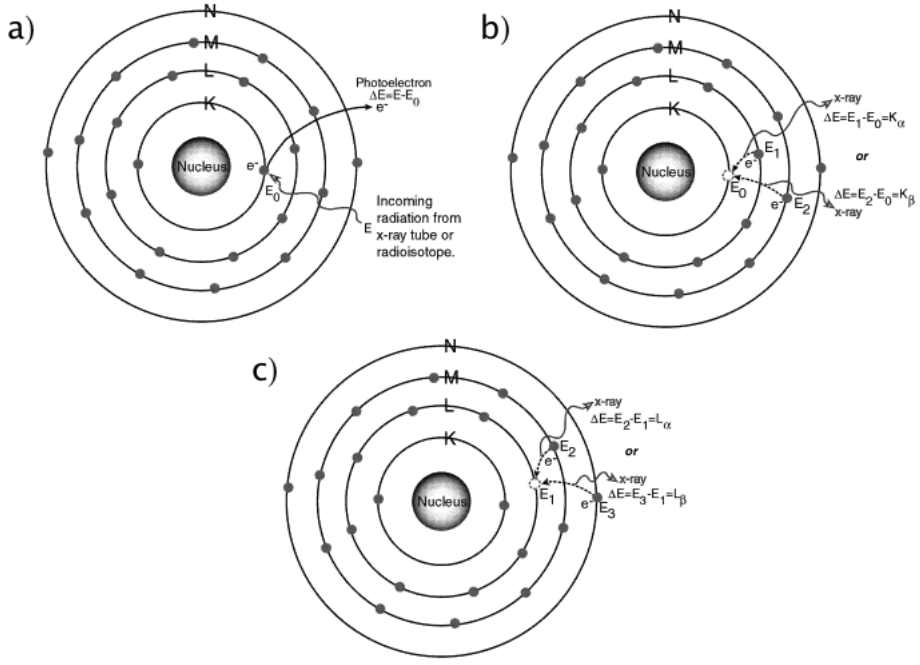

2 Procedures and Setup

The schematic of our experimental setup is shown in Fig. 2 below. We controlled both the X-ray source (Mini-X X-Ray Tube) and detector (Amp-Tek XR-100CR X-Ray Detector System and PX2CR Power Supply) through a desktop computer. The computer used Multi-Chanel Analyzer (MCA) Emulator software (MAESTRO) instead of using a standard pocket MCA. We controlled the number and the energy of the X-rays by adjusting the current and accelerating voltage, respectively. The source X-rays were then released through an aperture giving the X-rays an outgoing angle of approximately 120°. These X-rays then bombarded the samples and knocked out the inner electrons which consequentially produced the characteristic X-rays described in the introduction. These X-rays are then detected by the XR-100CR and then amplified by the PX2CR. The analog signals are also converted to digital signals for the computer to understand. [5]

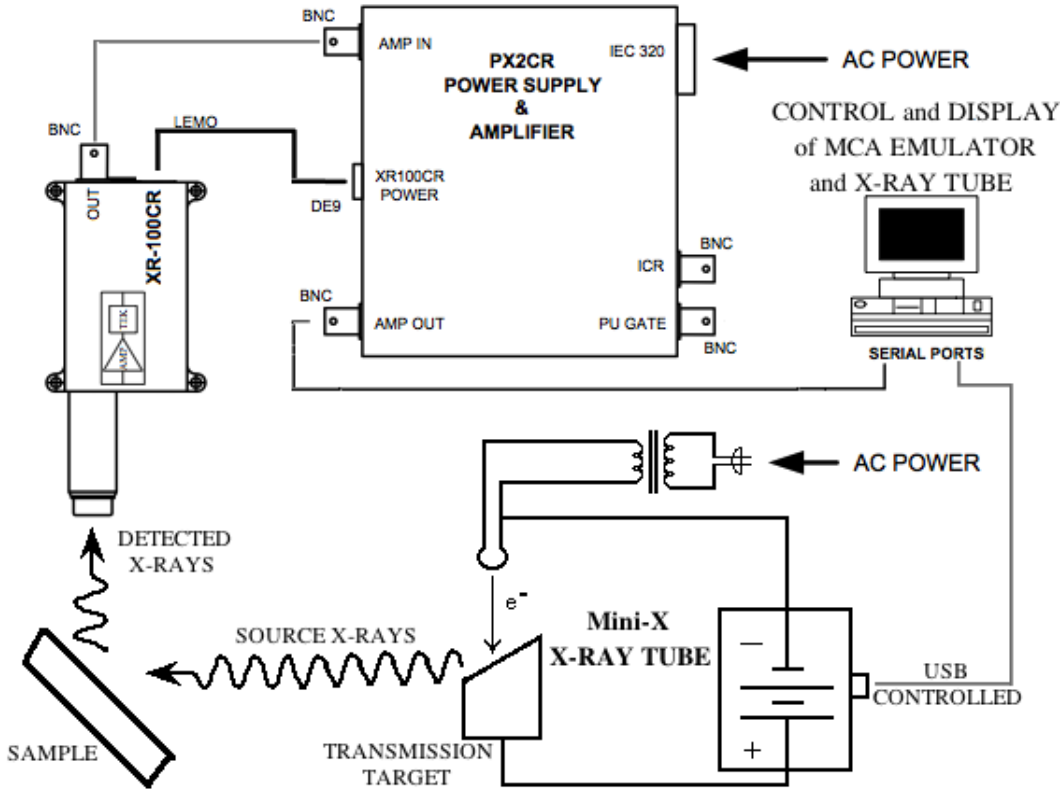

Figure 2: The schematic of our experimental setup. The connectors were BNC or LEMO. The Mini-X X-Ray Tube was USB controlled. We did not use the PU Gate or the ICR. [3] [5]

2.1 The X-Ray Source

According to the user manual the Mini-X X-Ray Tube is essentially a capacitor with a hole in one plate (a cathode and an anode with a small hole in it). We adjust the voltage across the capacitor to increase the momentum of electron. The higher the electron momentum when

it collides with the cathode filament (tungsten), then the higher energy X-ray is produced. The X-ray is produced in a vacuum so the window of its aperture is beryllium because it is very transparent to X-rays. Other materials would tend to absorb or scatter the X-rays. For the higher atomic number elements we increased the accelerating potential to produce energetic enough energies to knock out the tightly bound inner electrons. However, we did not increase the amperage to get more source X-rays.[3]

2.2 The X-Ray Detector

The Amp-Tek XR 100CR is a semiconductor-scintillator X-ray detector. The specifications can be found in the user manual. The scintillator is used to convert and multiply the incoming X-rays to visible light so that the photo-diode can register it as seen in Fig. 2 below. Once the X-ray is "softened" into lower energy light it passes through the pure silicon detector. X-rays by themselves do not create electron-hole pairs in the silicon detectors. However, they do knock out some electrons from their ground-state orbitals and it is the interaction between these electrons that create electron-hole pairs. Electron-hole pairs then separate (hole to n-type, electron to p-type) and create a voltage across the diode and current increases. This analog current is measured and converted to a digital signal for the computer to register. For the energies we observed the photoelectric effect is the main mechanism for converting photon energy to electron energy and hence analog voltage. [4]

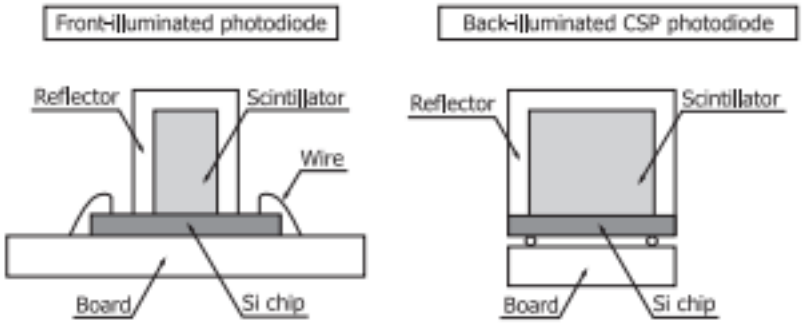

Figure 3: Schematic design of the semiconductor scintillator detector. Left is front illuminated and right is back illuminated. The reflector is made to trap the light created from the scintillator and focus it onto the silicon detector. The XR 100CR detector uses the back illuminated chip size package (CSP) photodiode to decrease the dead space. [4]

3 Data and Analysis

We have two types of data for our experiment. The first is the data that we collect from the MCA emulator during our X-ray fluorescence experiments. The second type is X-ray spectra data that has been collected previously and long been accepted as correct. We will use the "accepted" data as a reference for determining our known (mainly for calibration) and unknown samples. The finite bin size introduces an error on the order of the size of the bin. The bin size is dependent on the amplifier gain. We tried to keep the same gain to have as consistent results as possible. A few of the larger elements we had to increase the gain to get a stronger signal. However, this introduced more noise as you can see in our lead data. For more information on the transitions see appendix B.

3.1 The Known Samples

We had approximately ten known samples to choose from. We chose the following because of the high quality spectra we were observing. We observed significant noise specifically for the zirconium ($Z = 40$) and molybdenum ($Z = 42$) samples. At around 20 keV the signal of the X-rays also decreased significantly. Increasing the gain of the signal amplifier tended to just increase the noise and not the actual signal. This is why we began measuring the L lines with indium. The unknowns consist of one pure substance and two alloyed compounds. We present our X-ray spectra of all samples below by increasing atomic number.

3.1.1 Nickel (Z=28) and Copper (Z=29) K_α, K_β Lines

Nickel and copper are commonly found elements in nature. Their atomic numbers are 28 and 29, respectively. This means nickel has 28 electrons and copper has 29 electrons. Both elements orbitals are filled up to their M shell (in spectroscopic terms its $[\mathrm{Ar}]4s^2 3d^8$ and $[\mathrm{Ar}]4s^2 3s^9$). The larger peak of both elements X-ray spectra is the K_α peak while the smaller one is the K_β peak. Note that there was 3 times as many counts for the α transitions as there were for the β transitions. This is because of the shielding due to the L orbital electrons making a potential barrier for the M orbital electrons to cross to get to lower energy orbitals. We had nearly the exact spectra of the XRF Research Inc. X-ray fluorescence graphs.[6]

The bin size of nickel was $83eV$. This means the true value of the peak could be within $\pm 83eV$ giving our predicted values of the $K_\alpha = 7480 \pm 83.0eV$ and $K_\beta = 8230 \pm 83.0eV$. Comparing our nickel peak values to the established data (see appendix C) of $K_\alpha = 7478.15eV$ and $K_\beta = 8264.66eV$, we find we are within approximately $2eV$ and $34eV$, respectively, of the measured values. Our copper values were $K_\alpha = 8048 \pm 98.00eV$ and $K_\beta = 8833 \pm 98.00eV$, which were within $0.12eV$ and $72eV$, which was well within the bin size values. We notice for both nickel and copper the K_α values are much closer to established values than the K_β peaks. This could be due to the relative amplitudes of the peaks, as mentioned above. We have fit each of the tallest peaks to a gaussian and presented the data in the analysis section for further error analysis.

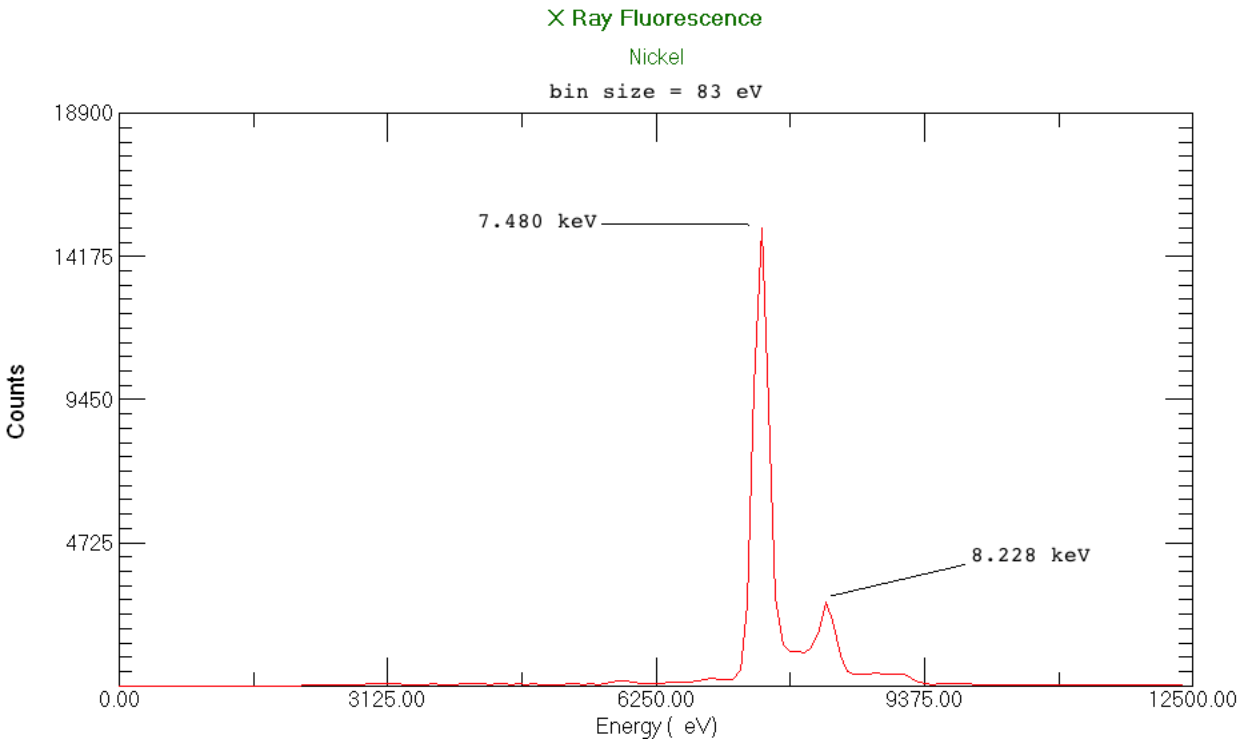

Figure 4: K line X-ray spectra of Nickel.

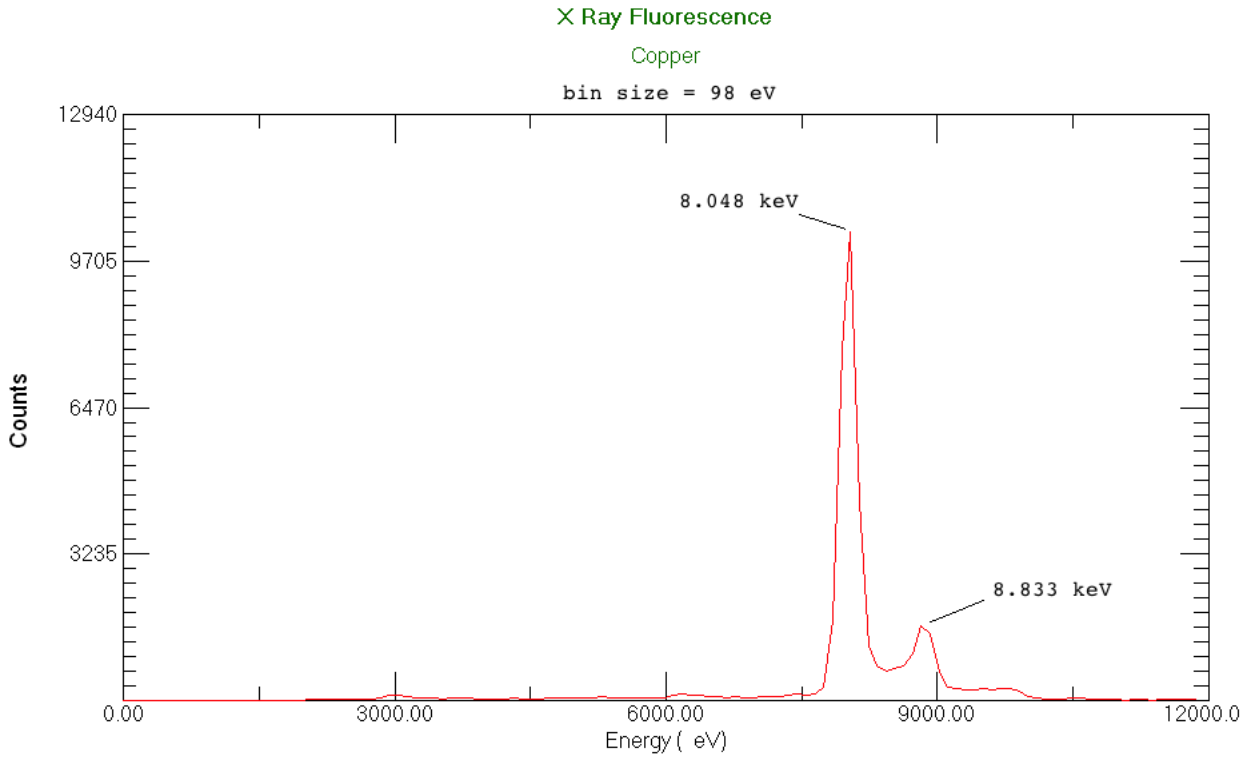

Figure 5: K line X-ray spectra of Copper

3.1.2 Indium (Z=49) L_α, L_β Lines

Indium is an important element, especially in solid state lighting. Since it belongs in III column of III-V semiconductors it is often used for doping in gallium nitride (GaN) based devices. It has a unique X-ray spectra because of its relatively close peaks. We compared our spectra to the XRF Research Inc. [6] data as seen in Fig. 6 below. The K lines are more distinct in the XRF Research Inc. data but we were unable to probe those energies without introducing significant noise. Comparing to the data tables given to us in the lab manual [1] as can been in appendix C and the XRF Research Inc. data we see that our data is within our accepted error (bin size= $82eV$) The taller peak ($E = 3.286$ keV) is the L_α line and the smaller ($E = 3.450$keV) is the L_β line.

Our values are then given as $L_\alpha = 3286 \pm 82.00eV$ and $L_\beta = 3450 \pm 82.00eV$, which are within $3eV$ and $37eV$, respectively, of the established data values (see appendix C). Analysis of the peak shape is given in the Further Analysis section.

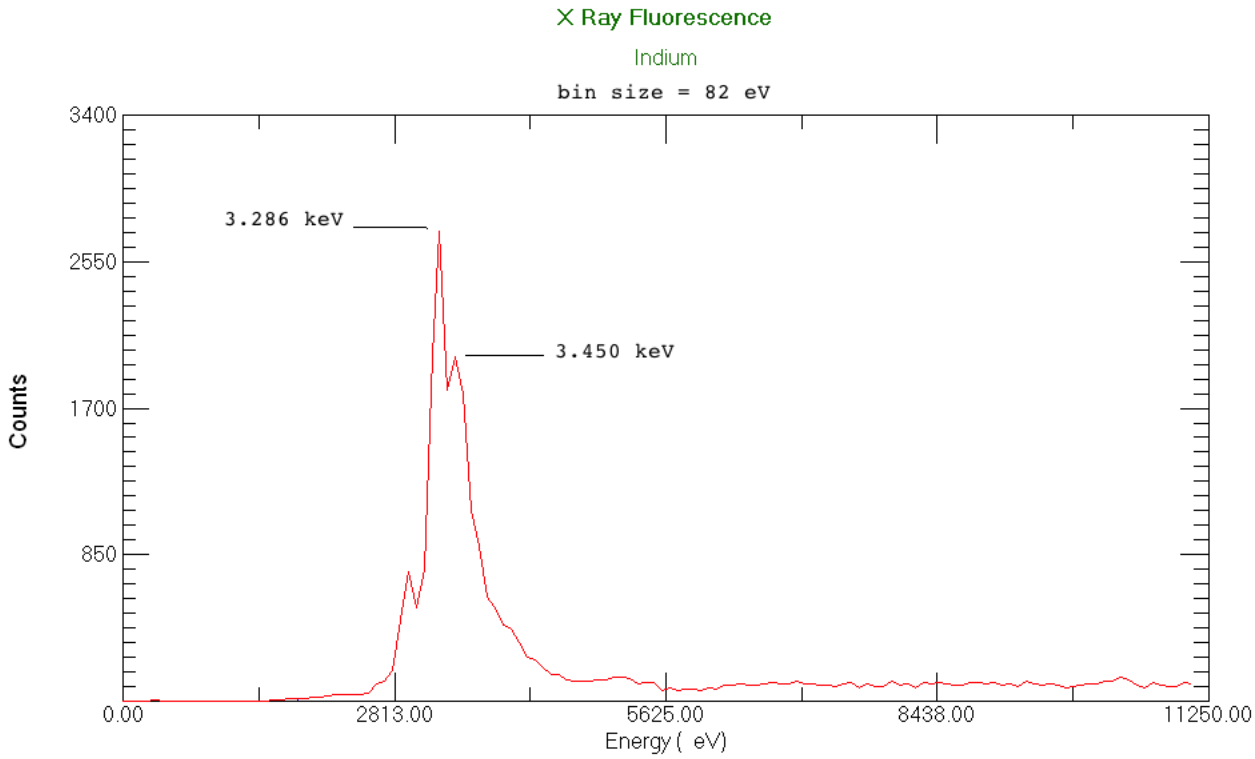

Figure 6: L line spectra of Indium. The smaller spectra is from XRF Research Inc. [6]

3.1.3 Gadolinium (Z=64) and Erbium (Z=68) L_ℓ, L_α, L_β, L_γ Lines

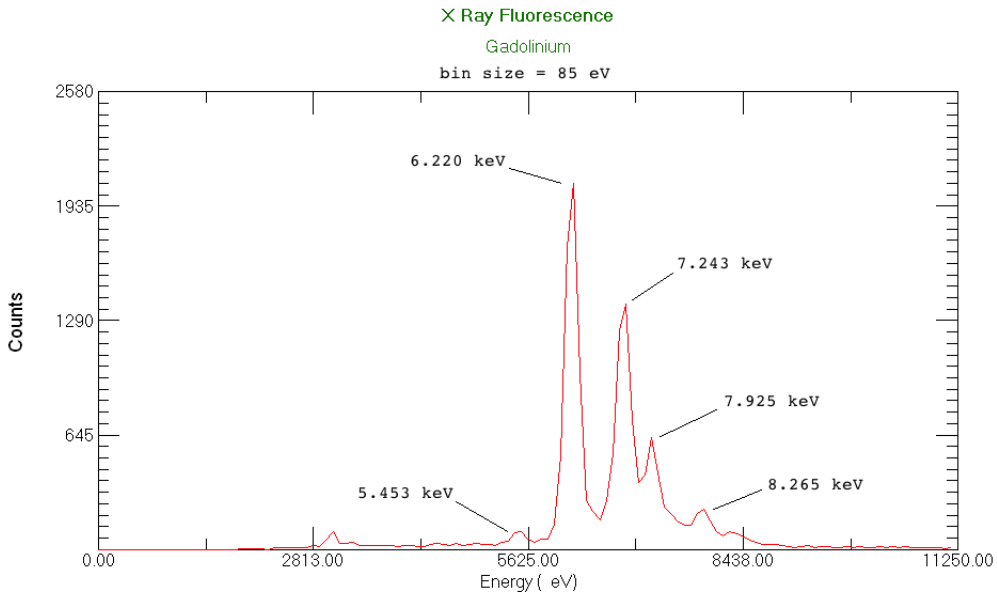

Figure 7: L line X-ray of Gadolinium .

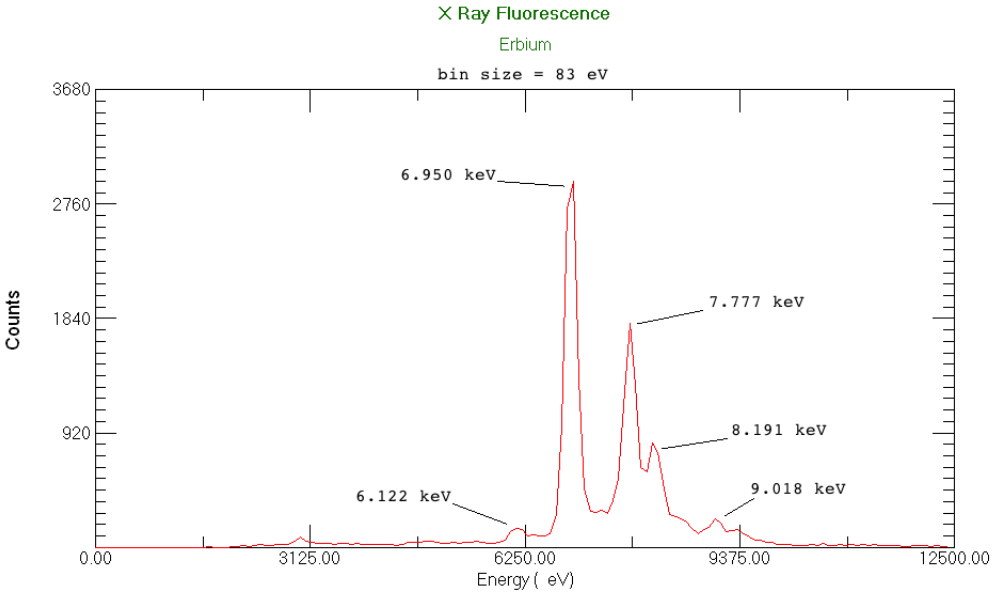

Figure 8: L line X-ray spectra of Erbium.

Both Gadolinium and Erbium are lanthanide or rare earth elements. However, this name is a misnomer created in the late 18th century, because lanthanide's are relatively common on earth. These elements fill up $4f$ electron shell or N orbital. This means that M, L, and K lines occur. The K lines are very high energy and was not observed for both elements. The first peak (lowest energy peaks) of both erbium and gadolinium are the L_ℓ lines. The next

lines are are in order of increasing energyL_α, L_β and L_γ. Here is a table of the peak values and corresponding expected values for the first lines gadolinium:

Gadolinium			
Line	$E_{measured}(eV)$	$E_{established}(eV)$	$\Delta E(eV)$
L_ℓ	5453	5360	107
L_α	6220	6057.2	162
L_β	7243	7102.8	140
L_γ	7925	7785.8	140

Here is a table of the peak values and corresponding expected values for the first lines of erbium:

Erbium			
Line	$E_{measured}(eV)$	$E_{established}(eV)$	$\Delta E(eV)$
L_ℓ	6122	6150	28
L_α	6950	6948.7	1.3
L_β	7777	7810.9	44
L_γ	9018	9089	71

We see that the gadolinium values are almost double the bin size. We believe this is due to being slightly uncalibrated, since it is approximately the same value off for all of our values. If we average the ΔE values we get approximately $137eV$, which is roughly the value that each peak is shifted from expected value. For the erbium values we see that the peak values are well within the bin size of the established data values. See the next section for analysis of peak shape.

3.1.4 Lead (Z=82) L_ℓ, L_α, L_β and L_γ Lines

Lead is a unique element. It is the largest non radioactive element. We use it for shielding from radioactivity in numerous applications. For Lead we began having issues getting rid of the noise. We present the background noise here as a reference. The peaks labeled in Fig. 9 are in order of increasing energy are L_ℓ, L_α, L_β, L_γ. Here is a table of the peak values and corresponding expected values for the first lines of lead:

Lead			
Line	$E_{measured}(eV)$	$E_{established}(eV)$	$\Delta E(eV)$
L_ℓ	9094	9180	86
L_α	10550	10551.5	1.5
L_β	12732	12613.7	119
L_γ	14551	14764.4	213

These values are well within our bin size of $364eV$. The L_γ line is the farthest off but this is due to the larger noise level in the higher energy data as can be seen in Fig. 9. The

rest of the noise is due to high level of amplification (hence large bin size). We took the lead data for the longest amount of time but had the lowest counts (approximately 80 for lead and closer to 2000 for other elements). We believe this is due to the inability of X-rays to penetrate and eject the inner electrons as easily as the lower Z elements. This allowed for more noise, as seen in Fig. 10, to be observed rather than actual signal.

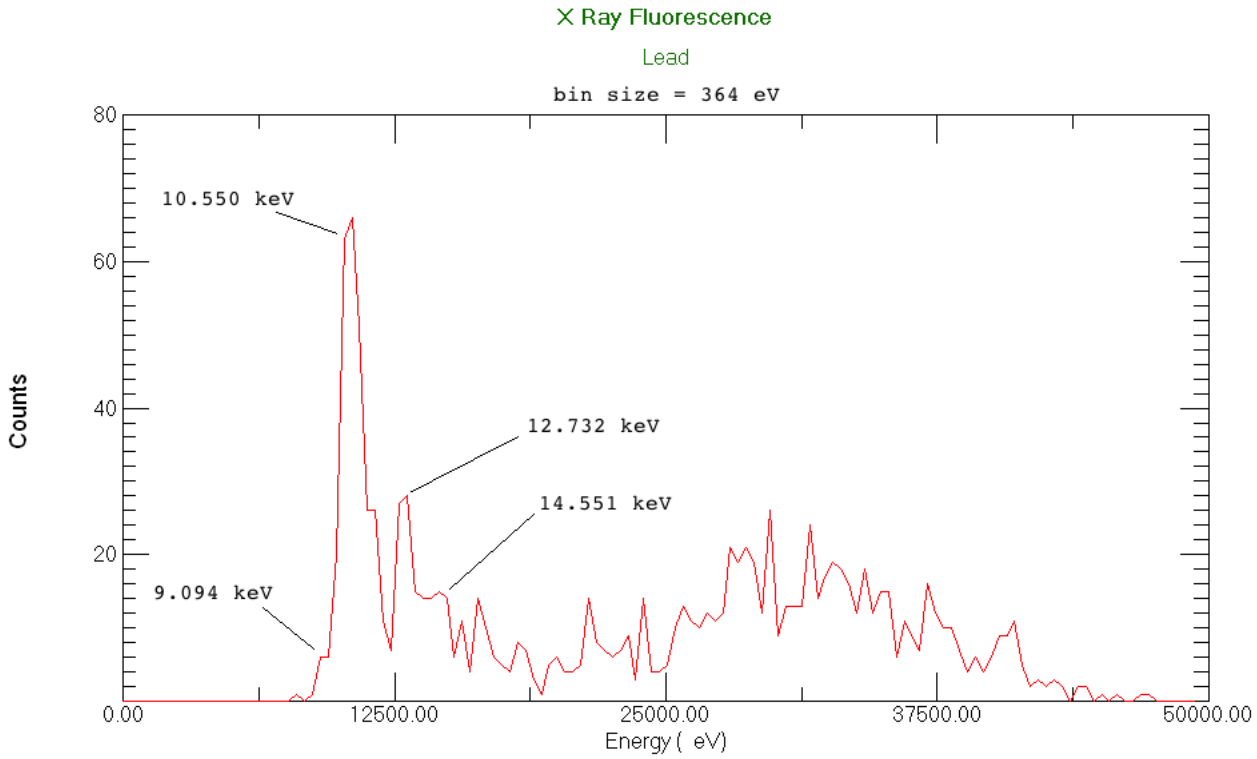

Figure 9: L line X-ray spectra of Lead.

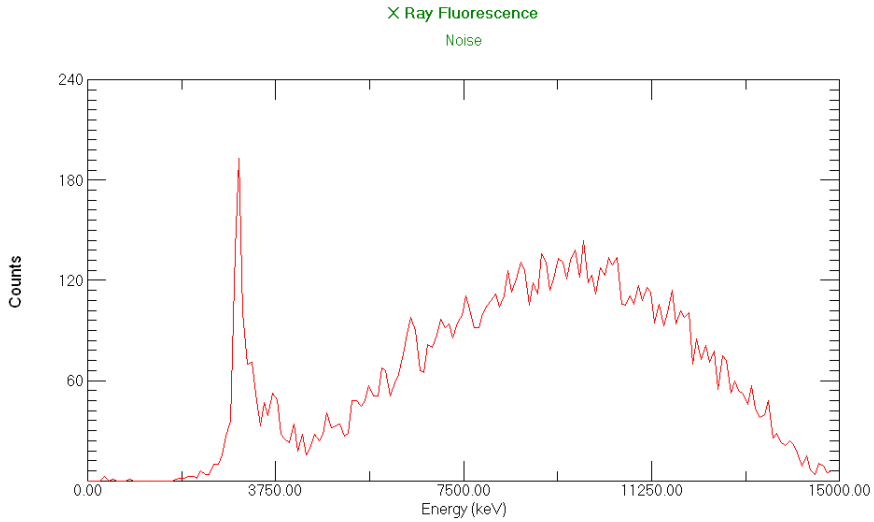

Figure 10: The noise without a sample.

3.2 The Unknown Samples

We found unknown materials in our laboratory and used X-ray fluorescence to determine the chemical composition of each substance.

3.2.1 Unknown Sample 1: Iron

Our first sample was a shiny piece of metal that was given as an unknown in the lab sample box. Comparing our peak positions to the given data tables we were able to quickly recognize this spectra as iron's. The first taller peak of Fig. 11 is $K_\alpha = 6456 \pm 83.00eV$ and the second labeled peak is $K_\beta = 7043 \pm 83.00eV$. The sample was small so we can see that noise was introduced in our data. Notice that the peak near $3300eV$ corresponds to the same peak as the first peak in the noise data (Fig. 10). We believe this $3300eV$ peak is due to the sample holder and/or stray X-rays from the X-ray source. Notice that it shows up consistently in almost all samples which would be indicative of either predicted sources of noise.

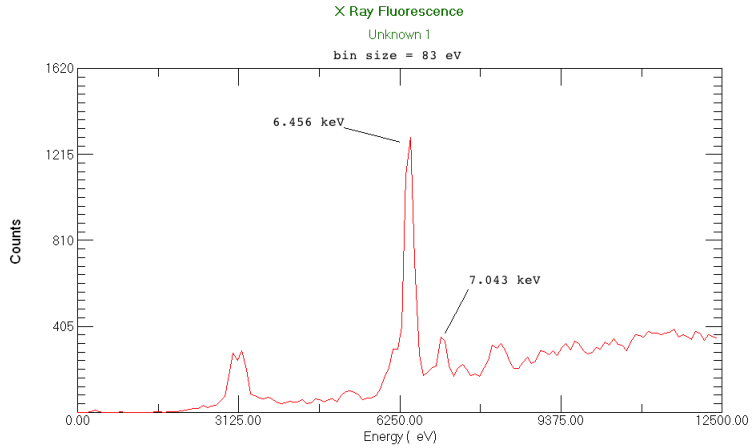

Figure 11: K line X-ray spectra of iron.

Comparing the measured value to the data tables ($K_\alpha = 6403.84eV$ and $K_\beta = 7057.98eV$) we see that the discrepancy in values is $53eV$ and $14eV$. These values are well within the bin size of this trial. There is a curious peak to the right of the K_β line which is rather diffuse and slightly double peaked. We could not pinpoint this peak as actual XRF signal. However, if it were it would most likely be the K_α, K_β lines of either nickel, copper, or cobalt.

3.2.2 Unkown Sample 2: Brass

This sample was a piece of a pipe connector. From the X-ray fluorescence spectra of Fig. 12 of the sample we saw four peaks. Comparing to our known sample data we determined the pipe was composition of copper and zinc. This is commonly known as the alloy brass. Note the small peak at $3200eV$, which is the due to background, because of the small dimensions of the sample. Our measured values are: $8050 \pm 84.00eV$, $8636 \pm 84.00eV$, $8888 pm 84.00eV$,

and $7043 \pm 84.00eV$. Since we measured both copper and nickel as our known samples one can compare peak values here with the values of the previous section. We see that all peaks are within the bin size of the data table values.

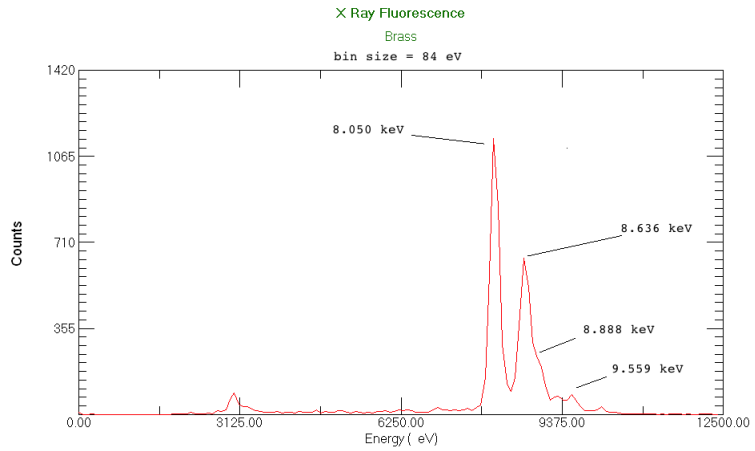

Figure 12: K line X-ray spectra of brass.

3.2.3 Unkown Sample 3: Stainless Steel

Our last unknown sample was a razor blade. The four peaks of X-ray fluorescence spectra indicated that it too was an alloy composed of two elements. Comparing the peak positions to our data tables we see that these peaks correspond iron and chromium. Steel is an alloy of multiple elements, but mainly carbon. Carbon however, does not have X-ray fluorescence lines above $2keV$. Due to the rise time discriminator of the amplifier carbon's peaks did not show up. Chromium is used to keep it from getting "stained". We see that the iron peaks in Fig. 13 are nearly identical to iron peaks of Fig. 11. The chromium values are $K_\alpha = 5450 \pm 84.00eV$ and $K_\beta = 5953 \pm 84.00eV$ which are within $35eV$ and $9eV$ of established peak values, respectively.

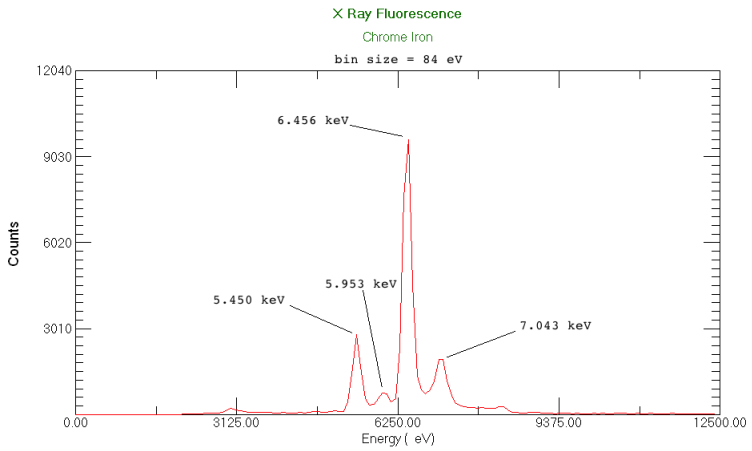

Figure 13: K line X-ray spectra of stainless steel.

4 Further Analysis

We used a data analysis program based in C and Python to fit the function

$$E(Z) = A(Z - \sigma)^2 \tag{1}$$

Where A is the energy scaling factor and σ is the screening term in Eq. 1. The quantity $(Z - \sigma)^2$ can be thought of as the effective atomic number. Since we only plotted the K_α lines we would expect that $\sigma = 1$ for the one electron still in the K shell. This function is called Moseley's Law after it's discoverer Henry Moseley. We assume that σ is not constant since for increasing Z amounts to increasing the number electrons around the atom. We plot two cases: $\sigma = 1$, and A a parameter, then both are parameters. For the latter we found the values of $A = 10.4 \pm 0.03$ and $\sigma = -0.99 \pm 0.04$ for the K_α lines. These sre intriguing values, especially the σ value. A negative σ value implies that the effective atomic number (total positive charge in nucleus) is actually increased by the presence of electrons in outer orbitals. This result is not intuitive and we do not have an adequate explanation of it, so we merely present here. However, comparing the free σ parameter result to the fixed one shows very little difference in the actual fits as can be seen in Fig. 14 and Fig. 15. This is because for large Z the difference between $Z - 1$ and $Z + 1$ is negligible, hence the reason that both fit the data very well.

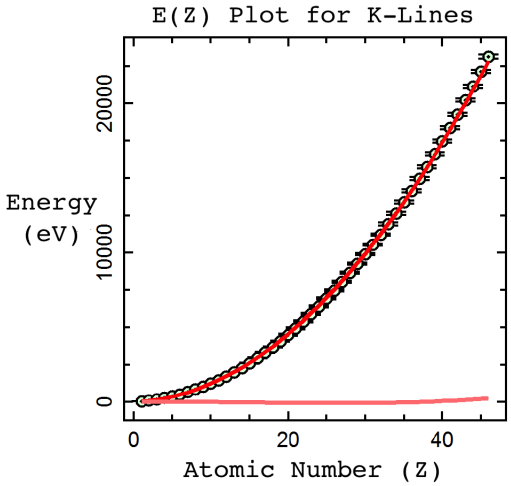

Figure 14: Moseley's law parameter fit with $\sigma = 1$. The red line is the fit function. The points are the data from the known tables. The light red is the difference between the fit and data points.

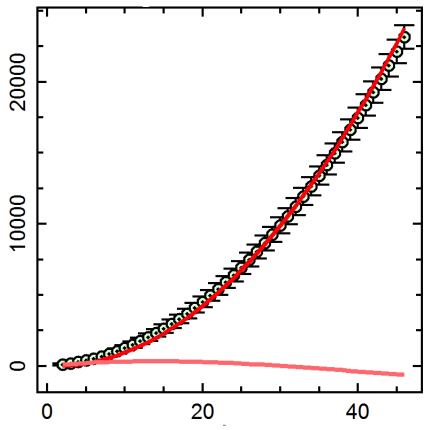

Figure 15: Moseley's law parameter fit with. The red line is the fit function. The points are the data from the known tables. The light red is the difference between the fit and data points. We found that σ is negative.

In regards to the A parameter we have found in both cases it has an approximate value of 10. This indicates that the K lines have a simple relationship to the atomic number which is $E(Z) \approx 10Z^2$. In reference to Fig. 14 and Fig. 15, they both have two solid lines, the (light red) line which is near the $E(Z) = 0$ represents the difference between the other solid line

(red) and the data points. See appendix A for some of our data analysis programs functions and parameters.

We have noted that there is huge discrepancy in peak values of the same elements. This goes against the our expected result that almost all peaks should have the same relative amplitude, since the transitions should produce a "waterfall effect" as mentioned previously. We have concluded that either β or L_α lines are less likely to occur because of the shielding effect. The inner electrons produce some sort of potential barrier that the outer electron has to overcome to make the transition.

All of our samples peak values have fallen within our bin size error estimate except for gadolinium. We reconciled this because eachpeak value was roughly off by the same amount, namely $140eV$. We assumed this was due to human error of our calibration of the MCA emulator, since it seemed like a systematic error. For all other peak values we were very pleased with the proximity to the established data table values. We noticed that the α peaks were often more accurate than the β peaks because the energy levels have slightly shifted once electrons have been ejected. This also leads to spread in the energy distribution in the peak energies. The changing of the bin sizes was due to the variance of the gain of the amplifier. We tried to keep the bin size around $85eV$ but for small signal samples like lead we increased the gain by more than a factor of 2. This is why the lead bin size is $283eV$. We believe this fact will have a correspondence to the Gaussian fits of the peak shapes. The larger the bin, the larger the standard deviation of the Gaussian distribution.

We present here the half width half maximum (HWHM)values (standard deviation of a Gaussian distribution) for a select number of our peak values:

Element	Line	HWHM	Maximum Amplitude (counts)	Bin Size (eV)
Iron	K_α	120	1360	83
Iron	K_β	100	305	83
Nickel	K_β	120	15000	83
Nickel	K_β	140	3500	83
Indium	L_α	250	2800	82
Erbium	L_α	175	2000	85
Erbium	L_β	250	1350	85
Lead	L_α	350	68	364
Lead	L_β	300	30	364

Examining the HWHM (or standard deviation) we found that there is a correspondence to bin size. Going back to our real time data (Fig. 16) we noted that most peaks had one bin as maximum value and two (on either side) as its roughly HWHM value. The plots presented above are the averages of these binned plots. Due to the large bin sizes the HWHM are inherently linked. Notice that the HWHM of most of the elements are approximately one and half times the bin size of the data. This means the center of the maximum bin is the peak and the adjacent bins outer edge is the point of HWHM.

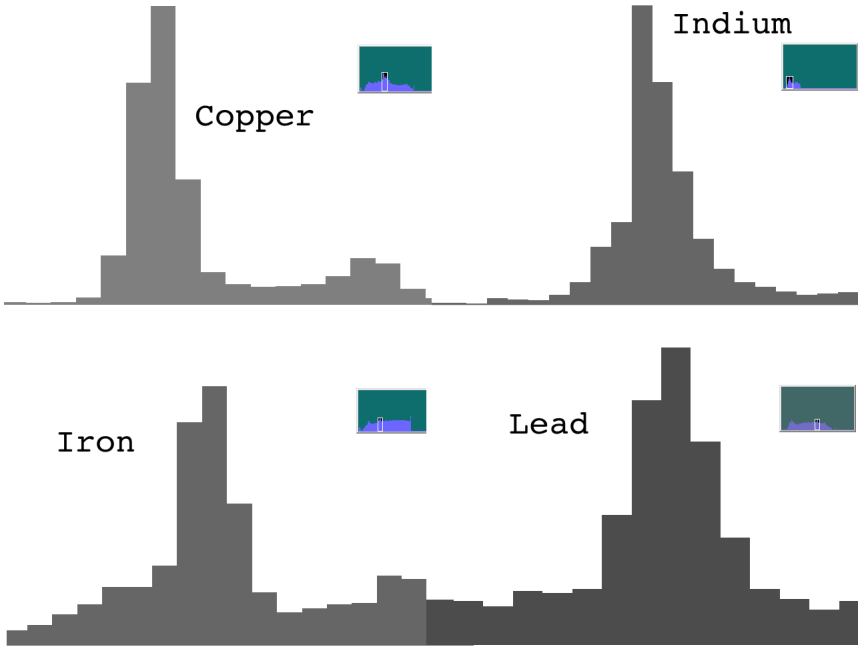

Figure 16: The bins of our histogram data for copper, indium, iron and lead.

From here we assumed that HWHM may not be the best way to estimate to the extrapolation of the plots presented from the raw data. Since the measured HWHM were inherently tied to the bin size and we could not determine the extrapolation algorithm we believe it is best to use bin size as our error bar. The precision of our peak positions (generally being well within the bin size of true value) confirm our bin size for error bar assumptions.

5 Conclusion

We have used X-ray fluorescence to confirm the energy spacings of various elements electron orbitals. We then calibrated our data to known samples and used X-ray fluorescence to determine the chemical composition of three unknown substances: iron, brass, stainless steel. Finally, we confirmed Moseley's Law by taking the known K_α lines and fitting them to Eq. 1 (See appendix A for the L_α line fits). We thought that the screening constant would be $\sigma = 1$ for the one electron in the K shell, however, we saw that σ goes as low as -1.34. We conclude that Moseley's discover was indeed an amazing leap forward for science and that his untimely death was horrific lost to society as a whole.

In regards to the experiment, we should have taken more XRF data and tried to fit our own data to the model. This would have been more insightful and rewarding because that is what Moseley did. We would also have liked to been able to understand the relationship between gain of the detector and the current and voltage of the source more completely. We

believe there is a delicate balance between the number of electrons and there acceleration in the X-ray source and the amplifier gain setting. However, we could not pinpoint the exact settings to maximize the signal and minimize the noise for all samples as can be seen in comparing lead to copper or gadolinium. This could have also been why we could not pick up the larger atomic number K lines, since as one can see for indium and up we only observed the L lines. For our unknown samples we picked objects with rather simple and bland chemical structure. If we could have redone the experiment we would have chosen more interesting unknown samples. Lastly, we would have liked to had a more diverse spread in atomic numbers of our known elements. We chose groups of elements due to limited resources. If we had done this we could have tried fitting our own data to Moseley's fit function (Eq. 1).

Due to the relative ease of the experimental setup, procedure, and analysis of the XRF lab we would have liked to seen a further inquiry into Moseley's fit function. As you can see in appendix A, we did go slightly further to investigate if the L lines had a similar fit. We could have also looked at α or β lines independently and investigated orbital transitions in more detail.

References

[1] George Brown, Sue Carter. Physics 134 Lab Manual. Winter 2014.

[2] Rutherford, Ernest. "Moseley, Henry Gwyn Jeffreys (18871915)." Rev. J. L. Heilbron. Oxford Dictionary of National Biography. Ed. H. C. G. Matthew and Brian Harrison. Oxford: OUP, 2004. Online ed. Ed. Lawrence Goldman. 28 Jan. 2014 http://www.oxforddnb.com/view/article/35125 .

[3] Amp-Tek. Mini-X User's Manual Rev B0

[4] Hamamatsu. Opto-semiconductor Handbook. at ¡http://jp.hamamatsu.com/sp/ssd/tech_handbook_en.

[5] Amp-Tek. Operating Manual XR-100CR X-Ray Detector System and PX2CR Power Supply/Shaper. Revision 13 October 2003.

[6] XRF Research Inc. http://www.xrfresearch.com/technology/xrf-spectra

[7] Amp-Tek Inc. Characteristic X-Rays. http://www.amptek.com/pdf/characteristic_xrays.pdf

[8] Lawrence Berkeley National Laboratory. X-Ray Data Booklet. October 2009. http://xdb.lbl.gov/xdb-new.pdf

A Fit Functions Using Privately Developed C and Python Data Shop Program

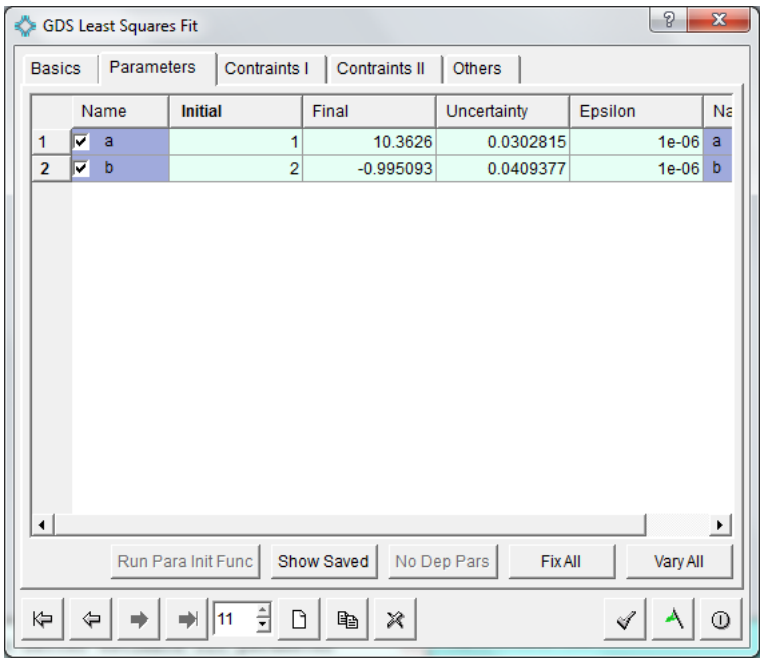

Figure 17: Screen shot of programs GUI. Final parameter values for K line fits with $a = A$, $b = \sigma$

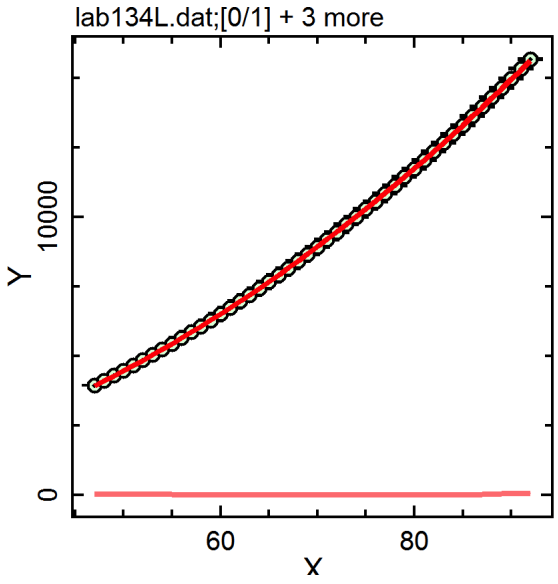

Figure 18: Moseley's law parameter fit with unconstrained parameters. The red line is the fit function. The points are the data from the known tables. The light red is the difference between the fit and data points. This is for L lines of elements $46 < Z < 82$.

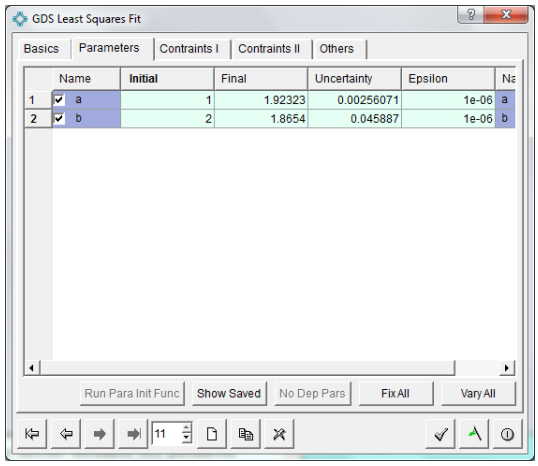

Figure 19: Screen shot of programs GUI. Final parameter values for L line fits with $a = A$, $b = \sigma$

B X-Ray Fluorescence Figures and Lines

Here are some nice figures from the Amp-Tek's Characteristic X-Rays documentation [7]. The first shows a detailed schematic of each possible schematic.

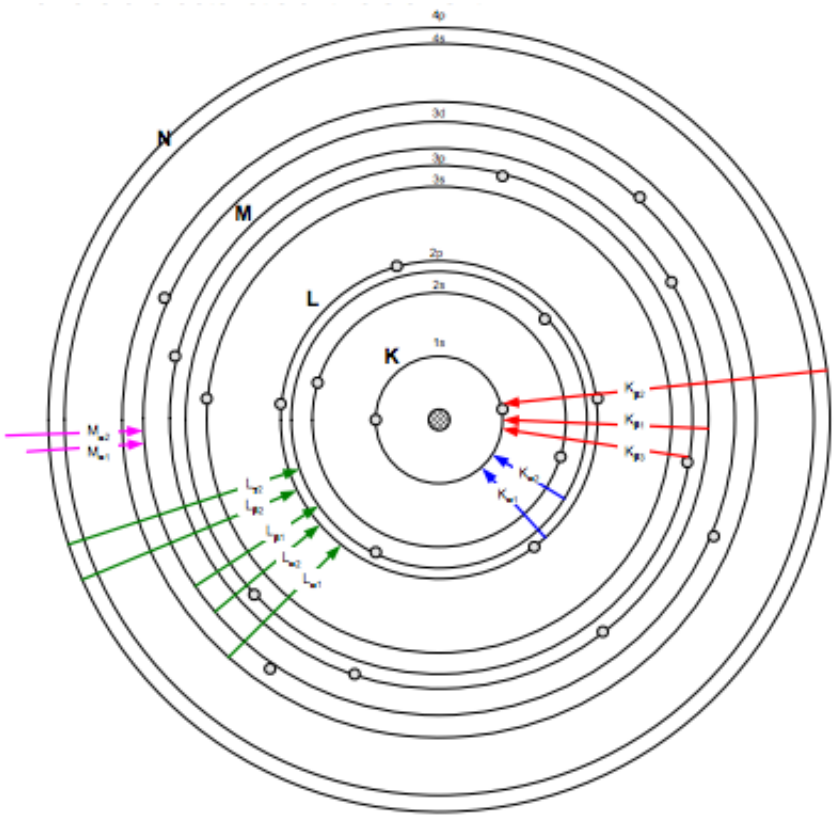

Figure 20: Diagram of electronic transitions. [7]

The corresponding X-ray fluorescence plots from Amp-Tek's Characteristic X-Rays documentation [7].

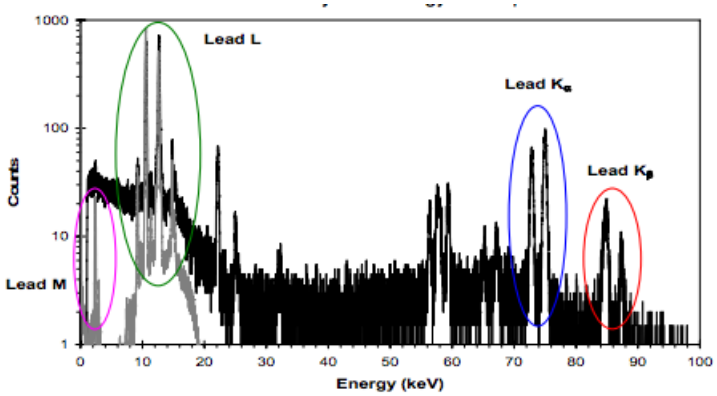

Figure 21: X-ray fluorescence plots of electronic transitions. [7]

Here is an easy to read figure of transitions with some extra information from Amp-Tek's Characteristic X-Rays documentation [7].

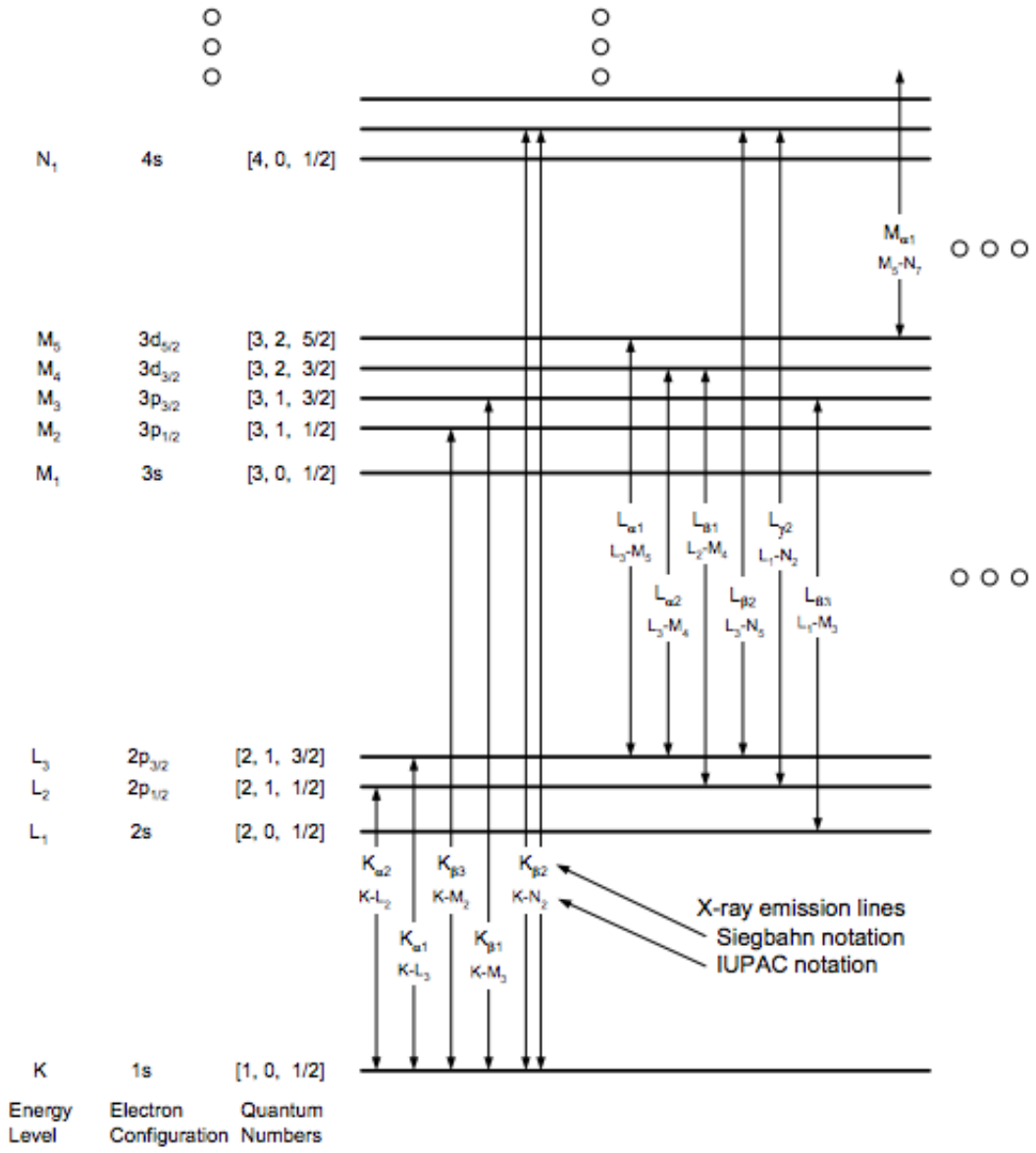

Figure 22: All Electronic transitions with X-ray emission lines. [7]

C X-Ray Emission Data

The following data has collected and compiled by researchers at Lawrence Berkeley's National Laboratory Center for X-ray Optics and Advanced Light Source. [8]

X-Ray Data Booklet Table 1-2. *Photon energies, in electron volts, of principal K-, L-, and M-shell emission lines.*

Element	$K\alpha_1$	$K\alpha_2$	$K\beta_1$	$L\alpha_1$	$L\alpha_2$	$L\beta_1$	$L\beta_2$	$L\gamma_1$	$M\alpha_1$
3 Li	54.3								
4 Be	108.5								
5 B	183.3								
6 C	277								
7 N	392.4								
8 O	524.9								
9 F	676.8								
10 Ne	848.6	848.6							
11 Na	1,040.98	1,040.98	1,071.1						
12 Mg	1,253.60	1,253.60	1,302.2						
13 Al	1,486.70	1,486.27	1,557.45						
14 Si	1,739.98	1,739.38	1,835.94						
15 P	2,013.7	2,012.7	2,139.1						
16 S	2,307.84	2,306.64	2,464.04						
17 Cl	2,622.39	2,620.78	2,815.6						
18 Ar	2,957.70	2,955.63	3,190.5						
19 K	3,313.8	3,311.1	3,589.6						
20 Ca	3,691.68	3,688.09	4,012.7	341.3	341.3	344.9			
21 Sc	4,090.6	4,086.1	4,460.5	395.4	395.4	399.6			

Table 1-2. *Energies of x-ray emission lines (continued).*

Element	$K\alpha_1$	$K\alpha_2$	$K\beta_1$	$L\alpha_1$	$L\alpha_2$	$L\beta_1$	$L\beta_2$	$L\gamma_1$	$M\alpha_1$
22 Ti	4,510.84	4,504.86	4,931.81	452.2	452.2	458.4			
23 V	4,952.20	4,944.64	5,427.29	511.3	511.3	519.2			
24 Cr	5,414.72	5,405.509	5,946.71	572.8	572.8	582.8			
25 Mn	5,898.75	5,887.65	6,490.45	637.4	637.4	648.8			
26 Fe	6,403.84	6,390.84	7,057.98	705.0	705.0	718.5			
27 Co	6,930.32	6,915.30	7,649.43	776.2	776.2	791.4			
28 Ni	7,478.15	7,460.89	8,264.66	851.5	851.5	868.8			
29 Cu	8,047.78	8,027.83	8,905.29	929.7	929.7	949.8			
30 Zn	8,638.86	8,615.78	9,572.0	1,011.7	1,011.7	1,034.7			
31 Ga	9,251.74	9,224.82	10,264.2	1,097.92	1,097.92	1,124.8			
32 Ge	9,886.42	9,855.32	10,982.1	1,188.00	1,188.00	1,218.5			
33 As	10,543.72	10,507.99	11,726.2	1,282.0	1,282.0	1,317.0			
34 Se	11,222.4	11,181.4	12,495.9	1,379.10	1,379.10	1,419.23			
35 Br	11,924.2	11,877.6	13,291.4	1,480.43	1,480.43	1,525.90			
36 Kr	12,649	12,598	14,112	1,586.0	1,586.0	1,636.6			
37 Rb	13,395.3	13,335.8	14,961.3	1,694.13	1,692.56	1,752.17			
38 Sr	14,165	14,097.9	15,835.7	1,806.56	1,804.74	1,871.72			
39 Y	14,958.4	14,882.9	16,737.8	1,922.56	1,920.47	1,995.84			
40 Zr	15,775.1	15,690.9	17,667.8	2,042.36	2,039.9	2,124.4	2,219.4	2,302.7	

41 Nb	16,615.1	16,521.0	18,622.5	2,165.89	2,163.0	2,257.4	2,367.0	2,461.8	
42 Mo	17,479.34	17,374.3	19,608.3	2,293.16	2,289.85	2,394.81	2,518.3	2,623.5	
43 Tc	18,367.1	18,250.8	20,619	2,424	2,420	2,538	2,674	2,792	
44 Ru	19,279.2	19,150.4	21,656.8	2,558.55	2,554.31	2,683.23	2,836.0	2,964.5	
45 Rh	20,216.1	20,073.7	22,723.6	2,696.74	2,692.05	2,834.41	3,001.3	3,143.8	
46 Pd	21,177.1	21,020.1	23,818.7	2,838.61	2,833.29	2,990.22	3,171.79	3,328.7	
47 Ag	22,162.92	21,990.3	24,942.4	2,984.31	2,978.21	3,150.94	3,347.81	3,519.59	
48 Cd	23,173.6	22,984.1	26,095.5	3,133.73	3,126.91	3,316.57	3,528.12	3,716.86	
49 In	24,209.7	24,002.0	27,275.9	3,286.94	3,279.29	3,487.21	3,713.81	3,920.81	
50 Sn	25,271.3	25,044.0	28,486.0	3,443.98	3,435.42	3,662.80	3,904.86	4,131.12	
51 Sb	26,359.1	26,110.8	29,725.6	3,604.72	3,595.32	3,843.57	4,100.78	4,347.79	
52 Te	27,472.3	27,201.7	30,995.7	3,769.33	3,758.8	4,029.58	4,301.7	4,570.9	
53 I	28,612.0	28,317.2	32,294.7	3,937.65	3,926.04	4,220.72	4,507.5	4,800.9	
54 Xe	29,779	29,458	33,624	4,109.9	—	—	—	—	
55 Cs	30,972.8	30,625.1	34,986.9	4,286.5	4,272.2	4,619.8	4,935.9	5,280.4	
56 Ba	32,193.6	31,817.1	36,378.2	4,466.26	4,450.90	4,827.53	5,156.5	5,531.1	
57 La	33,441.8	33,034.1	37,801.0	4,650.97	4,634.23	5,042.1	5,383.5	5,788.5	833
58 Ce	34,719.7	34,278.9	39,257.3	4,840.2	4,823.0	5,262.2	5,613.4	6,052	883
59 Pr	36,026.3	35,550.2	40,748.2	5,033.7	5,013.5	5,488.9	5,850	6,322.1	929
60 Nd	37,361.0	36,847.4	42,271.3	5,230.4	5,207.7	5,721.6	6,089.4	6,602.1	978
61 Pm	38,724.7	38,171.2	43,826	5,432.5	5,407.8	5,961	6,339	6,892	—
62 Sm	40,118.1	39,522.4	45,413	5,636.1	5,609.0	6,205.1	6,586	7,178	1,081

Table 1-2. *Energies of x-ray emission lines (continued).*

Element	Kα_1	Kα_2	Kβ_1	Lα_1	Lα_2	Lβ_1	Lβ_2	Lγ_1	Mα_1
63 Eu	41,542.2	40,901.9	47,037.9	5,845.7	5,816.6	6,456.4	6,843.2	7,480.3	1,131
64 Gd	42,996.2	42,308.9	48,697	6,057.2	6,025.0	6,713.2	7,102.8	7,785.8	1,185
65 Tb	44,481.6	43,744.1	50,382	6,272.8	6,238.0	6,978	7,366.7	8,102	1,240
66 Dy	45,998.4	45,207.8	52,119	6,495.2	6,457.7	7,247.7	7,635.7	8,418.8	1,293
67 Ho	47,546.7	46,699.7	53,877	6,719.8	6,679.5	7,525.3	7,911	8,747	1,348
68 Er	49,127.7	48,221.1	55,681	6,948.7	6,905.0	7,810.9	8,189.0	9,089	1,406
69 Tm	50,741.6	49,772.6	57,517	7,179.9	7,133.1	8,101	8,468	9,426	1,462
70 Yb	52,388.9	51,354.0	59,370	7,415.6	7,367.3	8,401.8	8,758.8	9,780.1	1,521.4
71 Lu	54,069.8	52,965.0	61,283	7,655.5	7,604.9	8,709.0	9,048.9	10,143.4	1,581.3
72 Hf	55,790.2	54,611.4	63,234	7,899.0	7,844.6	9,022.7	9,347.3	10,515.8	1,644.6
73 Ta	57,532	56,277	65,223	8,146.1	8,087.9	9,343.1	9,651.8	10,895.2	1,710
74 W	59,318.24	57,981.7	67,244.3	8,397.6	8,335.2	9,672.35	9,961.5	11,285.9	1,775.4
75 Re	61,140.3	59,717.9	69,310	8,652.5	8,586.2	10,010.0	10,275.2	11,685.4	1,842.5
76 Os	63,000.5	61,486.7	71,413	8,911.7	8,841.0	10,355.3	10,598.5	12,095.3	1,910.2
77 Ir	64,895.6	63,286.7	73,560.8	9,175.1	9,099.5	10,708.3	10,920.3	12,512.6	1,979.9
78 Pt	66,832	65,112	75,748	9,442.3	9,361.8	11,070.7	11,250.5	12,942.0	2,050.5
79 Au	68,803.7	66,989.5	77,984	9,713.3	9,628.0	11,442.3	11,584.7	13,381.7	2,122.9
80 Hg	70,819	68,895	80,253	9,988.8	9,897.6	11,822.6	11,924.1	13,830.1	2,195.3
81 Tl	72,871.5	70,831.9	82,576	10,268.5	10,172.8	12,213.3	12,271.5	14,291.5	2,270.6

82	Pb	74,969.4	72,804.2	84,936	10,551.5	10,449.5	12,613.7	12,622.6	14,764.4	2,345.5
83	Bi	77,107.9	74,814.8	87,343	10,838.8	10,730.91	13,023.5	12,979.9	15,247.7	2,422.6
84	Po	79,290	76,862	89,800	11,130.8	11,015.8	13,447	13,340.4	15,744	—
85	At	81,520	78,950	92,300	11,426.8	11,304.8	13,876	—	16,251	—
86	Rn	83,780	81,070	94,870	11,727.0	11,597.9	14,316	—	16,770	—
87	Fr	86,100	83,230	97,470	12,031.3	11,895.0	14,770	14,450	17,303	—
88	Ra	88,470	85,430	100,130	12,339.7	12,196.2	15,235.8	14,841.4	17,849	—
89	Ac	90,884	87,670	102,850	12,652.0	12,500.8	15,713	—	18,408	—
90	Th	93,350	89,953	105,609	12,968.7	12,809.6	16,202.2	15,623.7	18,982.5	2,996.1
91	Pa	95,868	92,287	108,427	13,290.7	13,122.2	16,702	16,024	19,568	3,082.3
92	U	98,439	94,665	111,300	13,614.7	13,438.8	17,220.0	16,428.3	20,167.1	3,170.8
93	Np	—	—	—	13,944.1	13,759.7	17,750.2	16,840.0	20,784.8	—
94	Pu	—	—	—	14,278.6	14,084.2	18,293.7	17,255.3	21,417.3	—
95	Am	—	—	—	14,617.2	14,411.9	18,852.0	17,676.5	22,065.2	—